

X-621-74-283

PREPRINT

NASA TM X- 70768

# THE EVOLUTION OF ELECTRON DENSITY AND TEMPERATURE DISTRIBUTIONS IN THE TOPSIDE IONOSPHERE DURING MAGNETIC STORMS

K. D. COLE  
J. A. FINDLAY

(NASA-TM-X-70768) THE EVOLUTION OF ELECTRON DENSITY AND TEMPERATURE DISTRIBUTIONS IN THE TOPSIDE IONOSPHERE DURING MAGNETIC STORMS (NASA) 24 p HC \$3.25

N75-10621

CSCL 04A G3/46

Unclas 53020

OCTOBER 1974



———— GODDARD SPACE FLIGHT CENTER ————  
GREENBELT, MARYLAND

**"This paper presents the views of the author(s), and does not necessarily reflect the views of the Goddard Space Flight Center, or NASA."**

**For information concerning availability  
of this document contact:**

**Technical Information Division, Code 250  
Goddard Space Flight Center  
Greenbelt, Maryland 20771**

**(Telephone 301-982-4488)**

THE EVOLUTION OF ELECTRON DENSITY AND TEMPERATURE  
DISTRIBUTIONS IN THE TOPSIDE IONOSPHERE DURING  
MAGNETIC STORMS\*

K. D. Cole\*\*

J. A. Findlay

October 1974

---

\*A portion of the material in this paper was presented at the AGU Annual Meeting 1970 (See Findlay & Cole, 1970)

\*\*On leave from La Trobe University Bundoora Vic. Australia 3083

GODDARD SPACE FLIGHT CENTER  
Greenbelt, Maryland

THE EVOLUTION OF ELECTRON DENSITY AND TEMPERATURE  
DISTRIBUTIONS IN THE TOPSIDE IONOSPHERE DURING  
MAGNETIC STORMS\*

K. D. Cole \*\*

J. A. Findlay

ABSTRACT

During geomagnetic storms the latitudinal distributions of electron density and temperature in the mid-latitude topside ionosphere are observed to change in a manner than can be related to the evolution of ring current particle populations as predicted theoretically earlier (Cole 1964; 1965). The region of auroral precipitation is characterized by correlated increases in electron temperature and density. Equatorwards of this region there is a broad belt of elevated electron temperatures and depressed electron densities which is usually much broader than any SAR-arc distinguishable from the ground, but which is nevertheless the same basic physical phenomenon. The changes of position of this belt can be related to prior bursts of geomagnetic activity and injection of ring current particles into the magnetosphere.

---

\*A portion of the material in this paper was presented at the AGU Annual Meeting 1970 (See Findlay & Cole, 1970)

\*\*On leave from La Trobe University, Bundoora Vic. Australia 3083

## CONTENTS

	<u>Page</u>
ABSTRACT . . . . .	iii
INTRODUCTION . . . . .	1
OBSERVATIONS . . . . .	5
DISCUSSION . . . . .	8
ACKNOWLEDGMENTS . . . . .	10
REFERENCES . . . . .	11

### ILLUSTRATIONS

<u>Figure</u>		<u>Page</u>
1	Schematic representation of the relation between ring current particles plasmapause and prior magnetic activity. (After Cole 1970 a, b) . . . . .	14
2	Histogram of variation of $K_p$ during the period October 28 - November 2, 1968 together with variation of position of inner edge of relatively disturbed magnetosphere (dashed line) during this period. . . . .	15
3	Composite of all electron density and temperature profiles versus magnetic invariant latitude for passes analyzed in the period of magnetic activity. . . . .	16
4	Plots of magnetic disturbance as function of invariant latitude together with topside $T_e$ and $n_e$ . The magnetic disturbance relates to the average over the previous five hours. . . . .	17
5	Plots of magnetic disturbance as function of invariant latitude together with topside $T_e$ and $n_e$ . The magnetic disturbance relates to the average over the previous five hours. . . . .	18

PRECEDING PAGE BLANK NOT FILMED

ILLUSTRATIONS (Continued)

<u>Figure</u>		<u>Page</u>
6	Plots of magnetic disturbance as function of invariant latitude together with topside $T_e$ and $n_e$ . The magnetic disturbance relates to the average over the previous five hours. . . . .	19
7	Plots of magnetic disturbance as function of invariant latitude together with topside $T_e$ and $n_e$ . The magnetic disturbance relates to the average over the previous five hours. . . . .	20
8	Plots of magnetic disturbance as function of invariant latitude together with topside $T_e$ and $n_e$ . The magnetic disturbance relates to the average over the previous five hours. . . . .	21
9	Plots of topside $T_e$ and $n_e$ against invariant latitude for pass 674 at 8 hrs. UT November 1 together with magnetic disturbance for prior burst of activity during period 1530 $\pm$ 2.5 UT on Oct. 31. . . . .	22
10	Plots of topside $T_e$ and $n_e$ against invariant latitude for pass 687 at 1000 hrs. UT on November 2 together with magnetic disturbance for prior burst of activity during period 1530 $\pm$ 2.5 UT on November 1. . . . .	23

THE EVOLUTION OF ELECTRON DENSITY AND TEMPERATURE  
DISTRIBUTIONS IN THE TOPSIDE IONOSPHERE DURING  
MAGNETIC STORMS

INTRODUCTION

During the onset of the main phase of a geomagnetic storm electric fields associated with magnetic fluctuations pump plasma from the outer to the inner magnetosphere. This process energizes plasma to form a ring current (Cole 1964). Frank (1967) has observed fluxes of energetic protons (up to 40 keV) in the magnetosphere sufficient to account for most of the ring current during two geomagnetic storms in 1966. More recently energetic  $O^+$  ions have been observed in the upper atmosphere at altitudes of about 800 km during geomagnetic storms over an L-value range of 2.4 to 9 (Shelley et al., 1972). Their fluxes are such that it appears that trapped  $O^+$  ions could contribute significantly to the energy of the ring current. Cole (1970 a,b) has shown a correlation consistent with earlier theory (Cole 1964, 1965) between the latitudinal distribution of geomagnetic fluctuations and the positions of the ring current and the plasmopause in the cold plasma. A SAR-arc observed from the ground during the storm of September 29, 1967 was related to the innermost L-shells of the relatively disturbed part of the magnetosphere. Figure 1 shows schematically a comparison of ground based measurements of magnetic fluctuations during the onset of the main phase of a magnetic storm, proton fluxes, and plasmopause during the recovery of the main phase as deduced earlier (Cole 1970 a,b).

The association between the magnetic fluctuations and the location of ring current particles during the storm is employed in the present paper to deduce the position of these particles. It is the purpose of this paper to compare the time evolution of the ring current position with the observed temperature and electron density distribution in the topside ionosphere. An identifiable SAR-arc represents only that portion of emission of atomic oxygen caused by excitation of the electrons in the high energy tail of the thermal distribution, which is discernible above the background of emission due to ionosphere recombination. The SAR-arc therefore is a limited manifestation of the more general phenomenon of the region of elevated electron temperatures and depressed electron densities (see Figure 3 of this paper and Figures 8 and 9 of Norton and Findlay 1969, Roble et al., 1971). The theory of Cole (1965) relied upon SAR-arc intensity measurements only for the purpose of estimating the electron temperature  $T_e$ . Since then, this parameter has become available from direct measurements and it is evident that this theory applies, a priori, equally well to the broad region of elevated  $T_e$  and depressed  $n_e$ . The exponential dependence of  $\lambda$  6300 Å emission together with its linear dependence on  $n_e$  and the atomic oxygen number density  $n(0)$  must explain the variability of  $\lambda$  6300 Å emission as a function of latitude. The most dominant of these parameters in this consideration is  $T_e$ .

It is clear that topside  $T_e$  and  $n_e$  data distinguish two substantially different regions. One is associated with auroral bombardment and field aligned electric currents where there are correlated increases of both  $T_e$  and  $n_e$  (see Findlay et al., 1969 and Figure 3 of this paper). The other region equatorwards of the



auroral region is one of increased  $T_e$  and generally depressed  $n_e$  (see Norton and Findlay 1969, Roble et al., 1971, Figure 3 of this paper). This is the region over which there is heat conduction from the magnetosphere. It is with the evolution in time during magnetic storms of this latter region that the present paper is concerned.

Cole (1965) suggested heat conduction to the ionosphere as a major sink of energy of energetic trapped particles. He proposed that as the trapped particles enter the inner magnetosphere coulomb collisions occur with the thermal plasma leading to a high background plasma temperature of approximately 1 ev. Particle-wave interactions have also been suggested as a mechanism to couple the energy of the ring current to the thermal plasma of the magnetosphere (Cornwall et al., 1971). This mechanism has recently been treated in a general fashion (Lin and Parks 1974). Conduction of heat occurs in the thermal plasma along the geomagnetic field to the lower ionosphere and neutral atmosphere and causes an elevation of the electron temperature there. Recently Newton et al., (1974) have suggested that enhanced electron temperatures in these regions may cause vibrational excitation of  $N_2$  which in turn can enhance the recombination rate in the ionosphere and cause some decrease of electron densities there. If the electron temperature is sufficiently great, emission at  $\lambda$  6300 Å from atomic oxygen may appear above the airglow background. However, it has been shown that excitation of atomic oxygen emissions accounts for only a very small fraction of the total energy loss of the electrons, most of which is lost through other

processes (Cole 1965) determined by the electron temperature. Therefore the distribution of electron temperature in the upper thermosphere provides the best means of examining the heat flow from the magnetosphere to the ionosphere during storms.

At the time of writing of his original paper Cole (1965) had only airglow measurements at his disposal for this purpose. Satellite measurements of electron density and temperature (Norton and Findlay 1969) and of ion densities and temperatures (Chandra et al., 1971) on field lines above the SAR-arc have been reported for the storm of 29 September 1967. These data are consistent with the conduction theory (see also Roble et al., 1971). Findlay (1969) reported that a narrow region of high electron temperature and a corresponding trough in electron density was a consistent feature found at altitudes of about 1200 km above observed SAR-arcs and that this feature moved in unison with the SAR-arcs through the storm period 31 October - 2 November 1968.

Using these data Roble et al., (1971) calculated 6300 Å emissions on the basis of heat conduction. They then compared the results to observations and found agreement. In this paper we use the electron temperature distribution at 1200 km as identification of the position of the SAR-arcs and the aforementioned geomagnetic fluctuation data as an indication of the position of the ring current. The evolution in U. T. of electron temperature distributions and the spatial distribution of geomagnetic fluctuations are studied here. These data in combination

support the theory of formation of the ring current (Cole 1964) and dissipation of its energy in the ionosphere (Cole 1965; Findlay and Cole 1970).

## OBSERVATIONS

The storm of October 28 - November 2, 1968 is selected for detailed study because of the amount of data available in the form of satellite observations of  $n_e$  and  $T_e$  and ground observation of SAR-arcs at midlatitudes and of surface magnetic disturbance data.

Figure 2 shows the variation of  $K_p$  through the period October 28 - November 2, 1968, the times of satellite passes and the intervals of observations of SAR-arcs. Figure 2 also shows how the position of the inner edge of the relatively disturbed magnetosphere varies during the storm period as determined from the latitude profiles of magnetic fluctuations. This position is determined from plots of magnetic fluctuations as a function of invariant latitude. In the diagrams in this paper we have chosen invariant latitude rather than L-value as coordinate because the satellite data is more uniformly distributed in the former coordinate. The magnetic data were derived from the 2.5 minute digitized ground based magnetic observations in the manner referenced above. The position of the inner edge of the magnetospheric proton fluxes is determined by drawing two straight lines (see Figures 4-9) one through the midlatitude disturbance and one along the steep rise of disturbance at higher latitudes. This rough procedure determines a point of intersection which, to within an accuracy of a

few degrees, indicates the latitude at which high-latitude disturbance commences.

We associate this surface latitude with the inner edge of observed proton fluxes in the magnetosphere on the same L-shell (Cole 1970 a,b, see Figure 1, this paper). Figure 3 shows the latitudinal distribution of electron temperature and density observed for the satellite passes indicated on Figure 2. There are ground based observations of the SAR-arc for each pass except numbers 640 and 652. For those two passes (as well as for the other) Roble et al., (1971) have calculated the position of the SAR-arc. The calculations and observation, agree for the passes 662, 674 and 687. The position of the SAR-arc as indicated by the electron temperature distribution (hatched areas in Figure 2) in passes numbers 640 and 652 is poleward of ground observatories, thus photometric confirmation of the position of the SAR-arc was not possible. Figures 4-8 combine plots of  $n_e$ ,  $T_e$ , and magnetic fluctuation profiles for five satellite passes approximately 24 hours apart. The magnetic disturbance profiles were determined in each case for the five hour period prior to the satellite pass and averaged over all longitudes.

It can be seen that for passes 640, 652 and 662 a good correlation exists between the  $n_e$ ,  $T_e$  features and the magnetic profile which as noted earlier (see Figure 1), is an indication of the position of the ring current. However, such a good correlation is not found for passes 674 and 687.

In Figures 9 and 10 the satellite data for passes 674 and 687 are replotted against magnetic profiles taken during the five hour period in each of the major bursts in activity as indicated by  $K_p$  prior to the satellite pass concerned. For pass 674 we use the magnetic profile for the period 1530 UT  $\pm$  2.5 hours on October 31. For pass 687 we use the magnetic profile for the period 1530 UT  $\pm$  2.5 hours on November 1. It is seen that good correlation is now also established for passes 674 and 687. In the case of pass 687 good correlation has also been found using several magnetic profiles taken during the active period from 1200 hours UT on November 1 to 0600 hours UT on November 2; whereas, correlation between  $n_e$ ,  $T_e$  features from pass 687 and magnetic profiles taken prior to the increase in  $K_p$  at 0800 UT on November 1 was found to be poor. Later on in November 5 and 6, the daily average of  $A_p$  subsided to very low values ( $\sim$  6 and 7) and during this time the  $n_e$ ,  $T_e$  profiles returned to normal, but on November 9 there was a small burst of magnetic activity. This burst had the effect (on pass 746) qualitatively similar to that described on passes 650, 652 and 662 and fitted the physical model tested in this paper. These observations can be summarized by saying the the  $n_e$ ,  $T_e$  features correlate both in position and time with a previous burst of new magnetic activity. The persistence of the  $T_e$  profile is then explained by the lifetime of the particles injected deep into the magnetosphere at the time of the burst of magnetic activity (Cole 1964, 1965).

Other general features in  $n_e$ ,  $T_e$  distributions are evident in the data. For example note in pass 687 the broad region of high  $T_e$  and depressed  $n_e$  extending

from  $\sim 45^\circ$  to  $\sim 60^\circ$ . In addition, there are observed anticorrelated spatial changes in  $T_e$  and in  $n_e$  in this region. This is distinct from the region in the vicinity of  $\Lambda \approx 70^\circ$  where both  $n_e$  and  $T_e$  increase and which has previously been identified with auroral precipitation (Findlay et al., 1969, Norton & Findlay 1969). We identify the former region as the region of heat conduction from the magnetosphere which contains a similarly broad distribution of particles (for example see Figure 2 of Frank 1967 and Figure 4 of Cole 1970 b).

#### DISCUSSION

The foregoing observations indicate that for all conditions of magnetic disturbance the location in L-space of heat conduction from the ring current may be determined from the position of the region of elevated  $T_e$  and depressed  $n_e$ . It is important to reiterate (Cole 1965, 1970 a, Cole et al., 1972) that the sink of energy for the ring current in the ionosphere is characterized by elevated  $T_e$  and that the SAR-arc as observed from the ground is only that portion of the region in which the value of  $T_e$  is sufficiently high that emission of 6300 Å photons resulting from thermal excitation is detectable above the general background intensity in this line. This paper shows that the region of heat flow from the ring current to the ionosphere often covers a region two to three times as broad as any SAR-arc as detected from the ground. Thus, for example in Figure 3, the width of the region of elevated  $T_e$  is about 1500 km (from  $L \approx 2$  to  $\approx 4$ ) whereas the SAR-arc as observed from the ground is only about 500 km wide (from  $L \approx 2.42$  to 2.76). Evidence bearing on this point can be found in earlier papers (Norton and Findlay 1969, Roble et al., 1971).

Theories of degradation of energy of the ring current must explain this broad region of elevated  $T_e$ . The theory of Cornwall et al., (1971) is restricted in application to a narrow region (or order 500 km) just equatorward of the L-value of the plasmopause.

The theory of Cole (1965) is not restricted in this way and predicts flow of heat into the ionosphere from the whole body of the ring current. The existence of cold plasma (a few ev) on field lines connected to the ring current is clear from the observations (Figure 3). The theory of Cornwall et al., (1971) requires that the density in the equatorial plane be of the order of  $100 \text{ cm}^{-3}$  before their mechanism is effective in heating the electron gas. Coulomb collisions, however, as employed in the theory of Cole (1965) continue beyond the region of equatorial plasmopause where the densities of cold plasma may be less. Energetic particles with pitch angles at the equatorial plane less than about  $45^\circ$  will exchange energy by Coulomb collisions mostly near their mirror points where the background electron density may be up to  $3 \times 10^3 \text{ cm}^{-3}$  (Cole 1974, to be published). These particles will provide heat flow to the ionosphere at L-values beyond the plasmopause.

We have demonstrated in the foregoing the spatial relationship of magnetic fluctuations and  $T_e$  profiles. Note the multiple peaks in  $T_e$  which may be related to the multiple bursts of magnetic activity. At this stage it should be mentioned that multiple SAR-arcs have been reported (Roach and Roach 1963). An examination of a wide range of data shows that in general the "pure" conduction

region is well separated from the precipitation region (Norton and Findlay 1969). These properties of the profiles persist even at quiet times and supports the contention that SAR-arcs exist at quiet times at high L-values (Cole 1965). Schaeffer and Jacka (1971) have reported observations of  $\lambda 6200\text{\AA}$  skyglow that may be interpreted in this manner. In this connection it is important to note that the data on  $T_e$  and  $n_e$  indicate no difference between the conduction region and the more limited region of the SAR-arc as observed from the ground.

Finally, within the resolution of the data available it is apparent that the conduction region featuring  $n_e$  and  $T_e$  appears immediately following each burst of magnetic activity. Moreover the data shows that the conduction region persists through the lifetime of the ring current. For example data on November 14, 1968 at 1200 UT when Dst is approaching zero the conduction region is still discernible.

#### ACKNOWLEDGMENTS

The assistance of Mr. L. Wharton with computations is greatly appreciated, as is the provision of magnetic data by the Data Center at NASA Goddard Space Flight Center. One of us (K. D. C.) is indebted to National Research Council of USA for the award of a Senior Post-Doctoral Research Associateship and to La Trobe University for leave of absence; his contribution forms part of a program of ionospheric research at La Trobe University which is funded by the Australian Research Grants Committee.



## REFERENCES

- Chandra S., E. J. Maier, B. E. Troy, Jr., and B. S. Narasingar Rao, "Subauroral red arcs and associated ionospheric phenomena" J. Geophys. Res 76, 920-925, 1971.
- Cole, K. D. "On the depletion of ionization in the outer magnetosphere during magnetic disturbances" J. Geophys Res 69, 3595-3601, 1964.
- Cole, K. D. "Stable auroral red arcs, sinks for energy of the Dst Main Phase" J. Geophys Res 70, 1689-1706, 1965.
- Cole, K. D. "Magnetospheric Processes Leading to Mid Latitude Auroras" Ann. Geophys., 26, 187-193, 1970 a.
- Cole, K. D. "Relationship of Geomagnetic Fluctuations to other Magnetospheric Phenomena" J. Geophys. Res 75, 4216-4223, 1970 b.
- Cole, K. D. "Coulomb collisions of ring current particles with magnetospheric plasma" to be published, 1974.
- Cole, K. D., F. Jacka and J. A. Thomas "Stable Auroral Red Arcs" The Australian Physicist, June Issue, 87-90, 1972.
- Cornwall, J. M., F. V. Coriniti and R. M. Thorne "Unified Theory of SAR-arc formation at the Plasmapause" J. Geophys. Res 76, 4428-4445, 1971.

- Findlay, J. A. "Electron Temperature and Density Measurements above the SAR-arc of October 29 - November 1, 1968" EOS Trans AGU 50, 648, 1969 (Abstract).
- Findlay, J. A., P. L. Dyson, L. H. Brace, A. J. Zmuda, and W. E. Radford "Ionospheric and Magnetic Observations at 1000 kilometers during the geomagnetic storm and aurora of May 25-16, 1967." J. Geophys Res 74, 3705-3712, 1969.
- Findlay, J. A. and K. D. Cole "Correlation of ionospheric electron temperature and density features with fluctuations in geomagnetic activity." EOS Trans AGU 51, 378, 1970 (Abstract).
- Frank, L. A. "On the extraterrestrial ring current during geomagnetic storms" J. Geophys. Res 72, 3753-3767, 1967.
- Lin, C. S., and G. K. Parks "Further discussion of the cyclotron instability" J. Geophys. Res 79, 2894-2897, 1974.
- Newton, G., J. C. G. Walker, and P. H. E. Meijer "Vibrationally excited nitrogen in SAR-arcs and its effect on ionospheric recombination" J. Geophys. Res. 79, 3807-3818, 1974.
- Norton, R. B., and J. A. Findlay "Electron density and temperature in the vicinity of the 29 September 1967 middle latitude red arc." Planet. Space Science 17, 1867-1877, 1969.

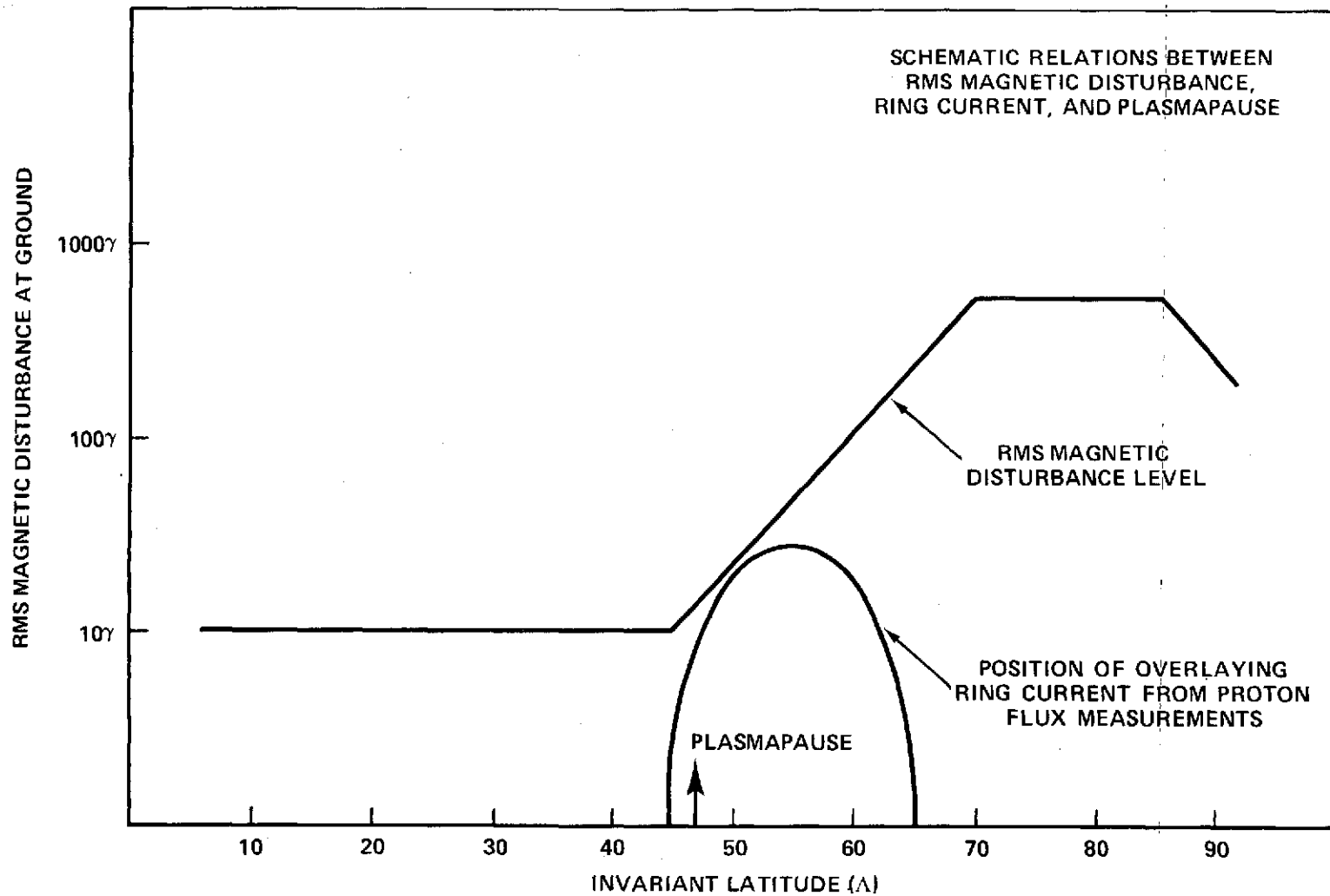


Figure 1. Schematic representation of the relation between ring current particles plasmopause and prior magnetic activity. (After Cole 1970 a,b)

$K_p$ , POSITION OF RING CURRENT, TIME OF  
ALOUETTE II DATA AND PERIODS OF  
SAR-arc OBSERVATION AT  $\Lambda \approx 50^\circ$   
OCT 28-NOV 2, 1968

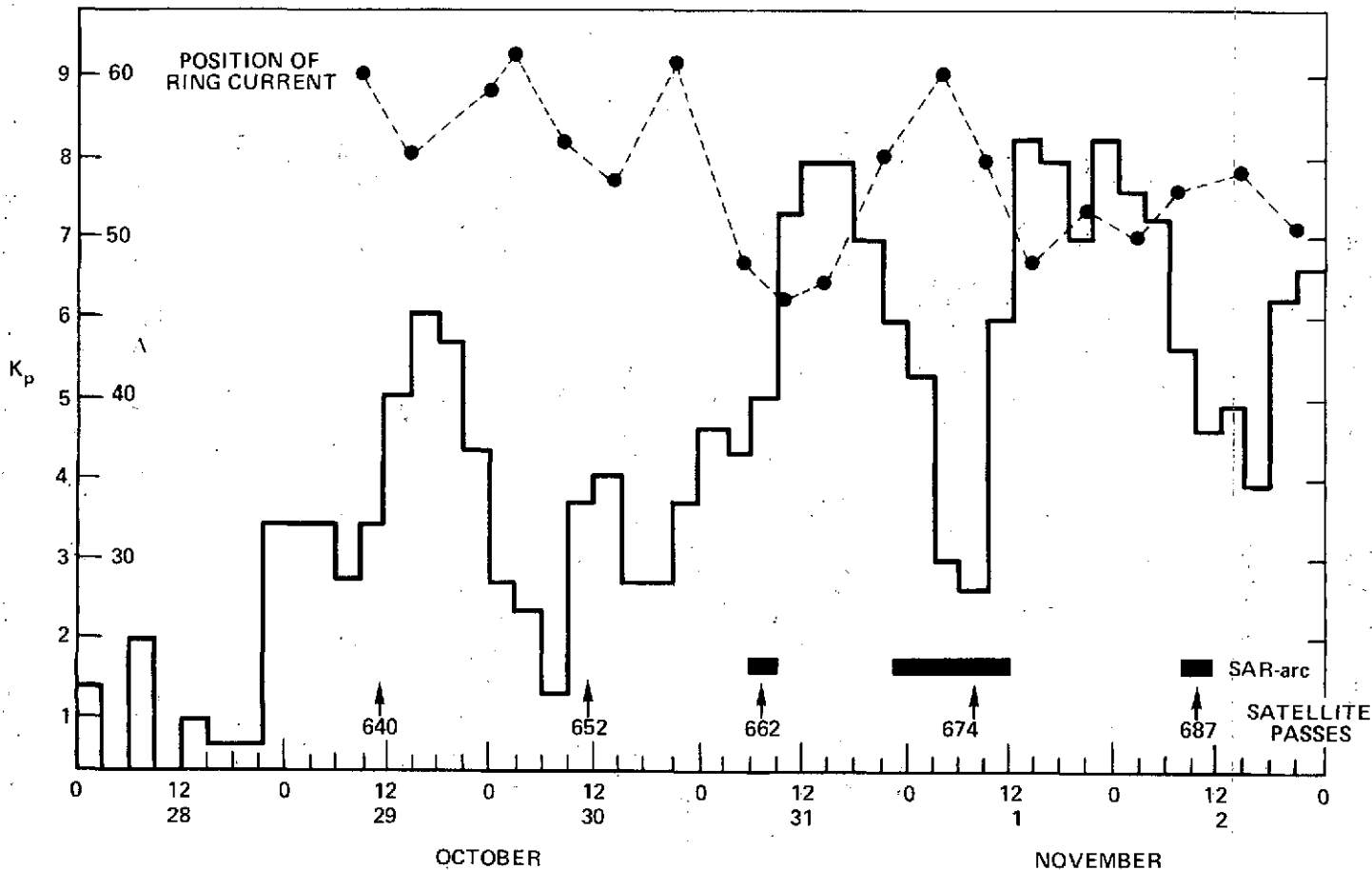


Figure 2. Histogram of variation of  $K_p$  during the period October 28 - November 2, 1968 together with variation of position of inner edge of relatively disturbed magnetosphere (dashed line) during this period.

$T_e$ ,  $N_e$  AND CALCULATED AND OBSERVED  
 POSITION OF SAR-ARC VS.  $\Lambda$  AT 1 DAY  
 INTERVALS 29 OCT. - 2 NOV. 1968  
 HGT = 1200 KM  $\pm$  400 KM LT  $\approx$  0330 HRS

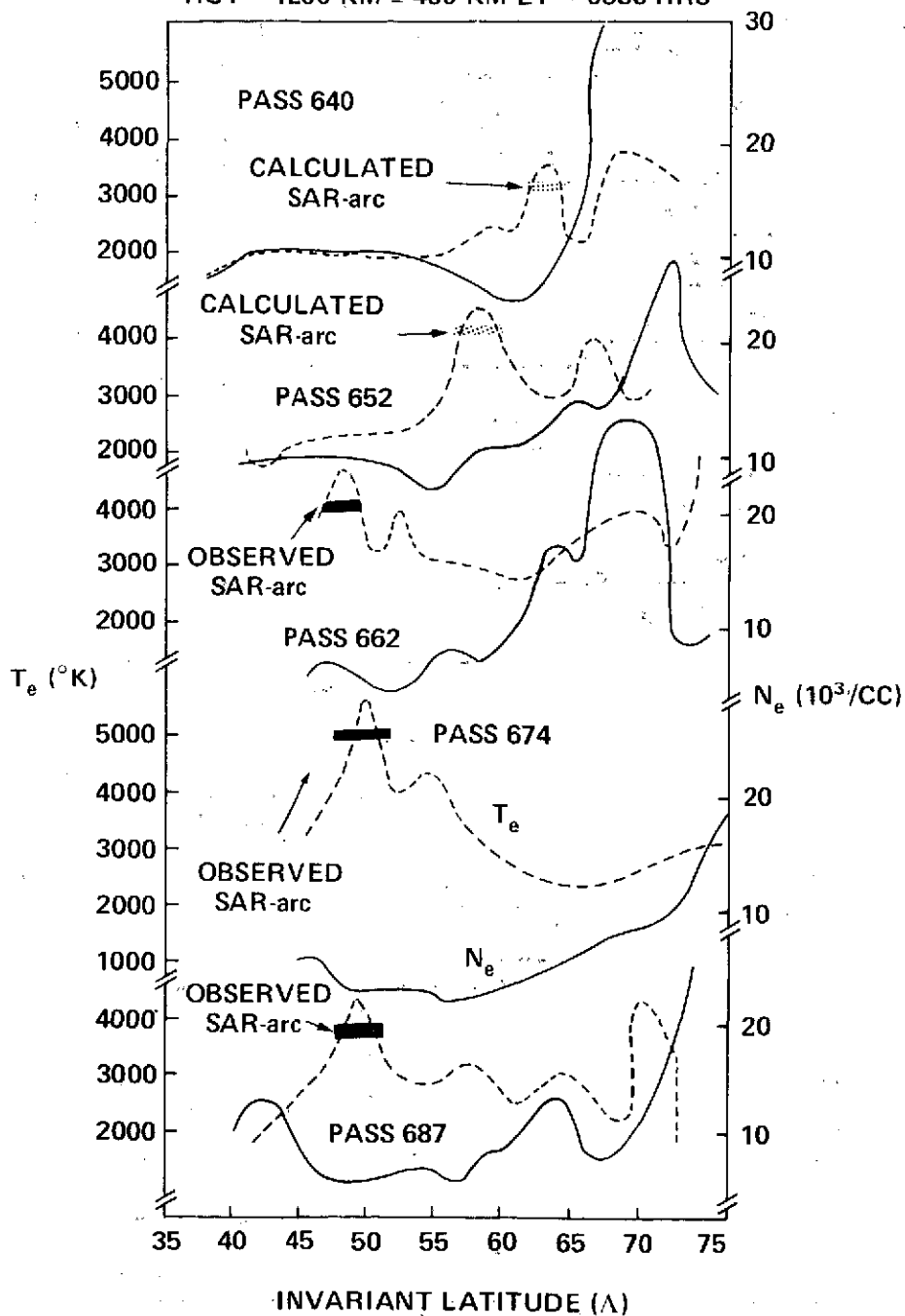


Figure 3. Composite of all electron density and temperature profiles versus magnetic invariant latitude for passes analyzed in the period of magnetic activity.

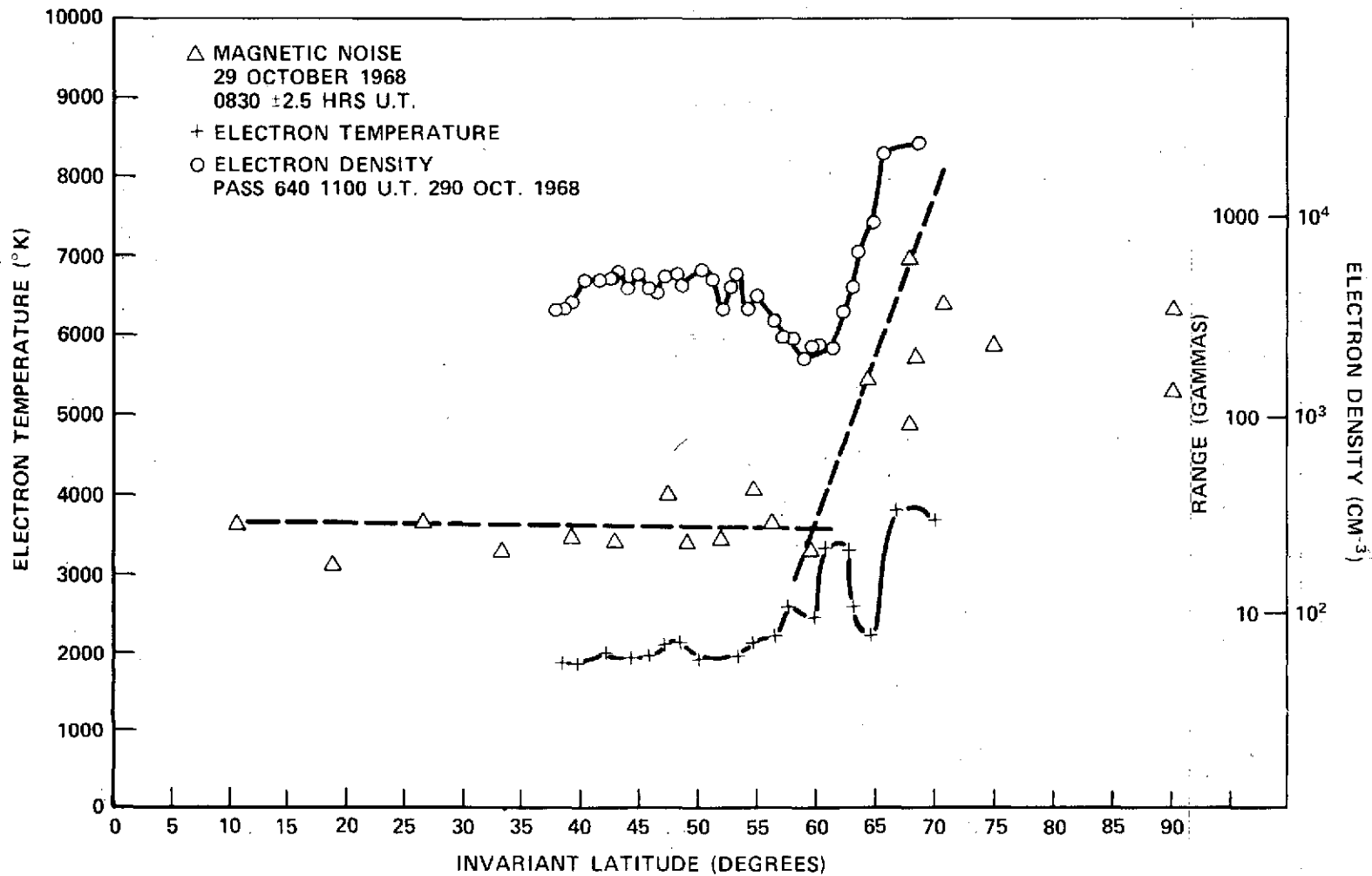


Figure 4. Plots of magnetic disturbance as function of invariant latitude together with topside  $T_e$  and  $n_e$ . The magnetic disturbance relates to the average over the previous five hours.

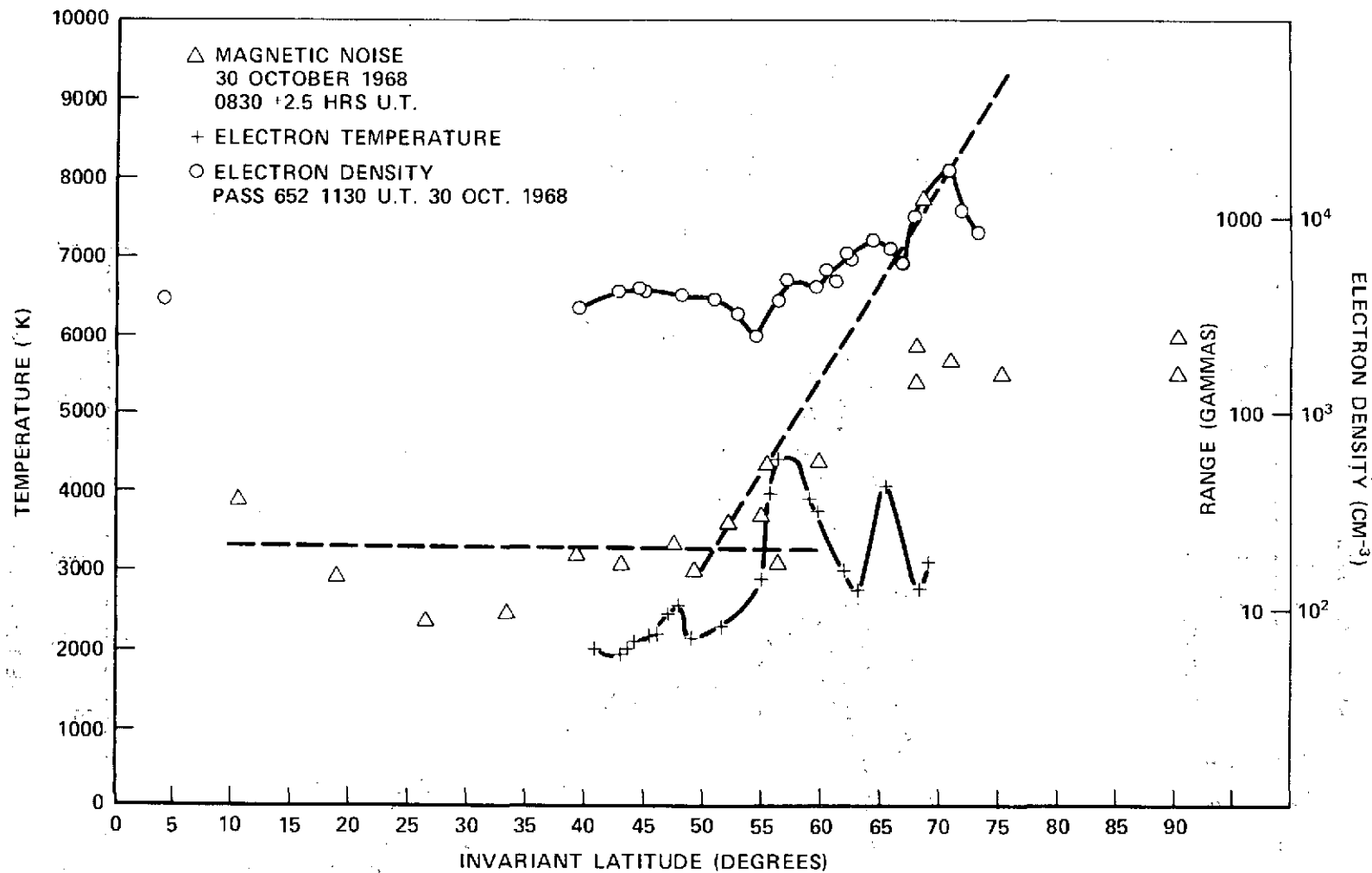


Figure 5. Plots of magnetic disturbance as function of invariant latitude together with topside  $T_e$  and  $n_e$ . The magnetic disturbance relates to the average over the previous five hours.

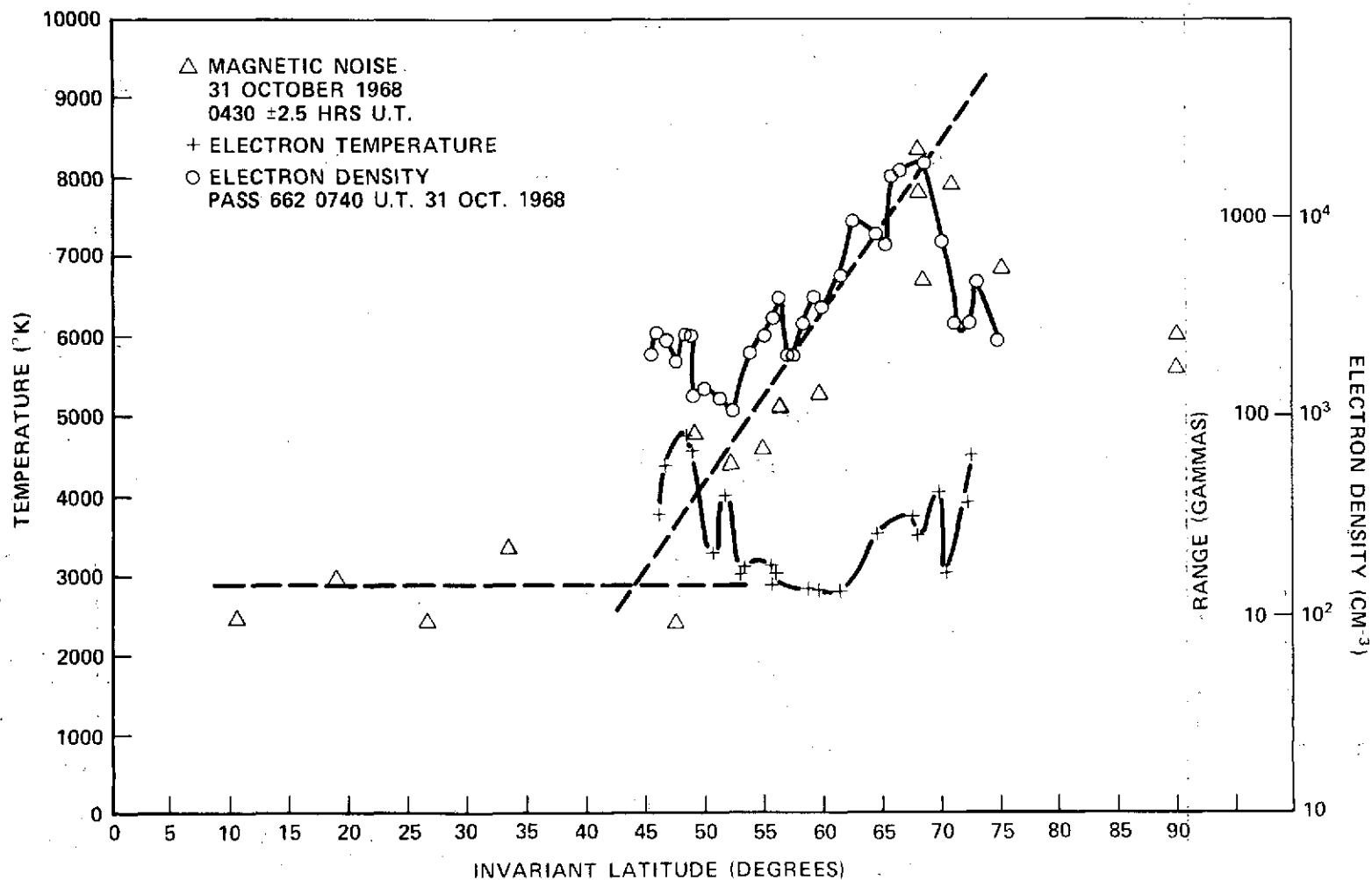


Figure 6. Plots of magnetic disturbance as function of invariant latitude together with topside  $T_e$  and  $n_e$ . The magnetic disturbance relates to the average over the previous five hours.



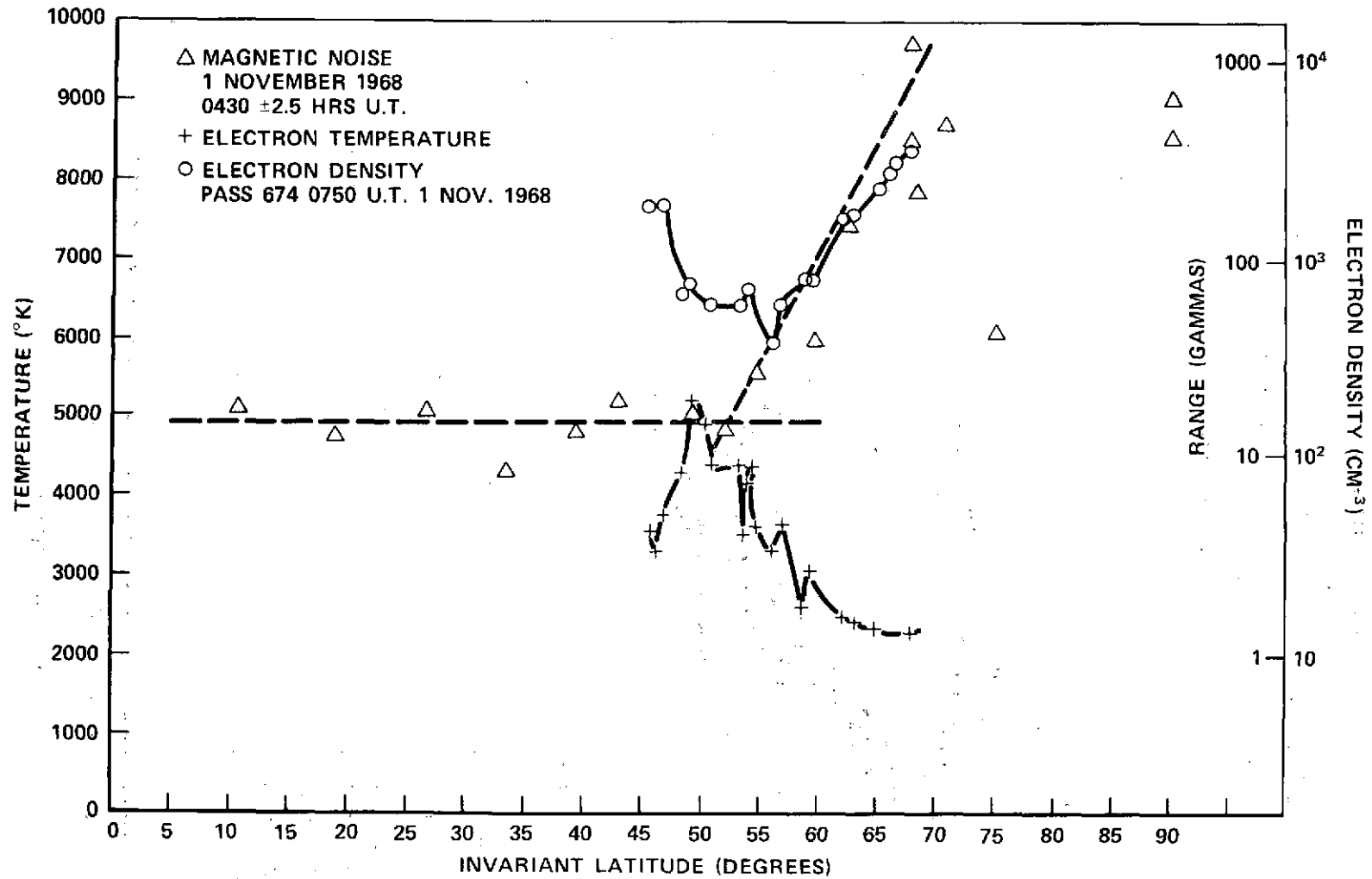


Figure 7. Plots of magnetic disturbance as function of invariant latitude together with topside  $T_e$  and  $n_e$ . The magnetic disturbance relates to the average over the previous five hours.

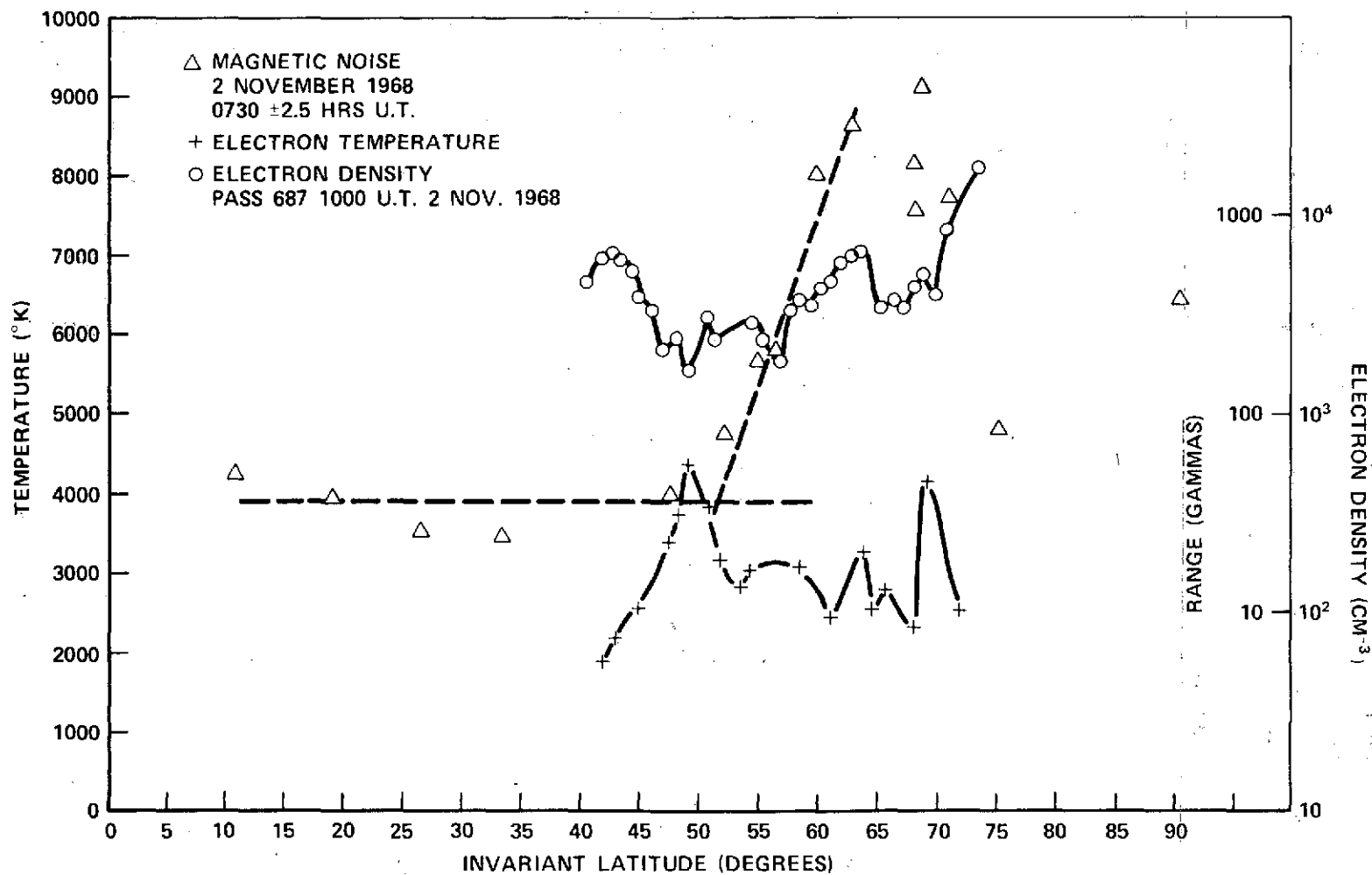


Figure 8. Plots of magnetic disturbance as function of invariant latitude together with topside  $T_e$  and  $n_e$ . The magnetic disturbance relates to the average over the previous five hours.

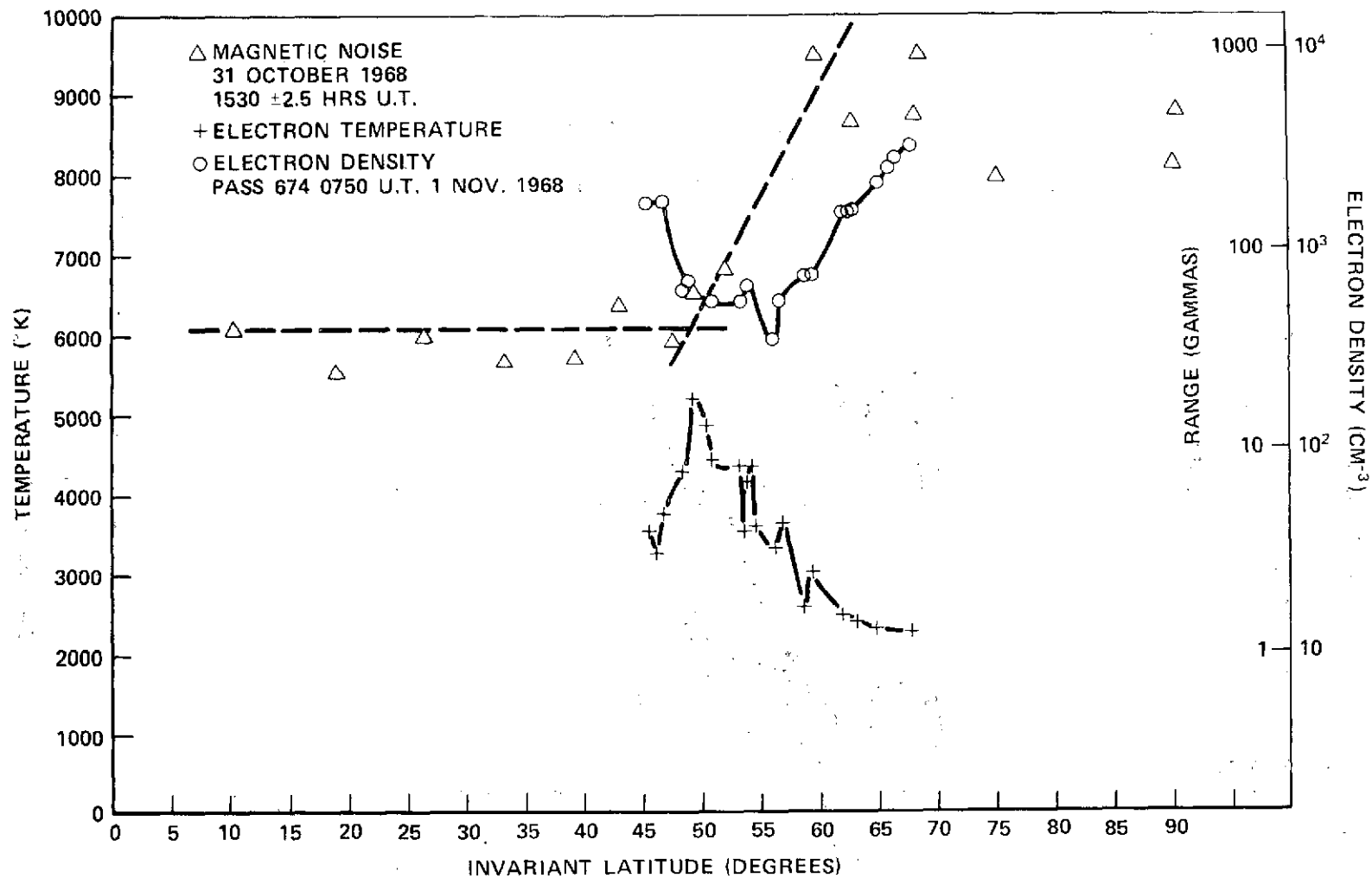


Figure 9. Plots of topside  $T_e$  and  $n_e$  against invariant latitude for pass 674 at 8 hrs. UT November 1 together with magnetic disturbance for prior burst of activity during period 1530  $\pm$  2.5 UT on Oct. 31.

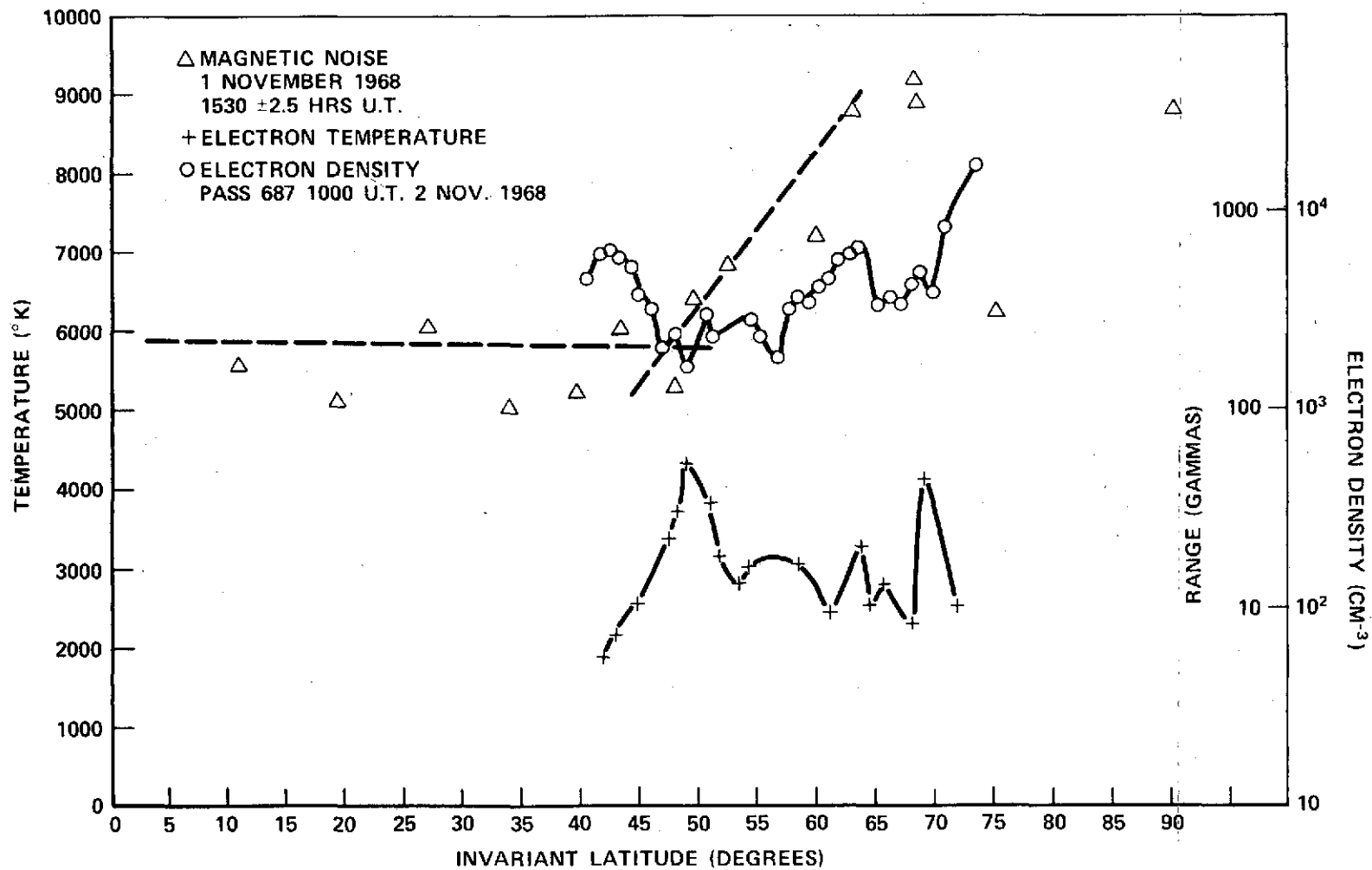


Figure 10. Plots of topside  $T_e$  and  $n_e$  against invariant latitude for pass 687 at 1000 hrs. UT on November 2 together with magnetic disturbance for prior burst of activity during period 1530  $\pm$  2.5 UT on November 1.